



# A luminous off-on probe for the determination of 2,6-pyridinedicarboxylic acid as an anthrax biomarker based on water-soluble cadmium sulfide quantum dots

Xiaoqing Li<sup>1</sup> · Lei Deng<sup>1</sup> · Fanghui Ma<sup>1</sup> · Minghui Yang<sup>1</sup>

Received: 27 October 2019 / Accepted: 11 April 2020 / Published online: 23 April 2020  
© Springer-Verlag GmbH Austria, part of Springer Nature 2020

## Abstract

A fluorescence off-on sensing platform was developed based on thioglycolic acid-stabilized cadmium sulfide quantum dots (CdS QDs) as fluorescence probe for the sensitive and selective detection of 2,6-pyridinedicarboxylic acid (DPA) in spores. The fluorescence emission intensity of the quantum dots at 650 nm when excited at 460 nm was first quenched by mixing with europium ions ( $\text{Eu}^{3+}$ ) and then recovered after the addition of DPA. The interaction of DPA with  $\text{Eu}^{3+}$  relieved the quenching effect of  $\text{Eu}^{3+}$  toward CdS QDs. As the DPA concentration increases, the color of the probe changes from colorless to red. The method exhibits a wide linear range from 1 to 120  $\mu\text{M}$  for DPA determination, with a detection limit of 0.2  $\mu\text{M}$ . The CdS QDs based nanoprobe was successfully applied for sensitive determination of DPA released from bacteria spores. In this case, the detection limit is  $3.5 \times 10^4 \text{ CFU} \cdot \text{mL}^{-1}$ .

**Keywords** *Bacillus anthracis* · Bacteria spores · 2, 6-Pyridinedicarboxylic acid · CdS quantum dots · Fluorescence recovery

## Introduction

Anthrax, the pathogen of which is anthrax bacillus, is a serious infectious diseases that threat to human health [1]. Once infected with anthrax bacillus, the spores of anthrax bacillus will enter the organism and multiply rapidly to form a capsule and release toxin [2]. More dangerously, people will die within 36 h if they inhaled more than  $10^4$  spores. So the prevention of anthrax have always been one of the focus of clinical medical research [3, 4].

Anthrax bacillus will be devitalized using disinfectant and some conventional sterilization methods. However, anthrax bacillus spores are highly resistant to high temperature, radiation, dryness, extreme pH, and other adverse conditions, so that they can survive for decades in the external environment

[5]. The strong stress resistance mainly depends on the highly dehydrated and high density of 2,6-pyridinedicarboxylic acid (DPA) and its calcium salts (Ca-DPA) in the core area and cytoplasm of spores [6]. DPA, accounting for 5–15% of the dry mass of spores, is therefore an essential component in spores and is often chosen as a marker for spores germination analysis [7].

Effective detection of *Bacillus anthracis* spores is an important way for prevention and treatment of anthrax. Dormant spores may germinate when the surrounding micro-environment is favorable for their growth. They may eventually convert back into growing cells, with duration time of 20–30 min. The process of spores germination is accompanied by release of DPA, the concentration of which corresponded to the number of spores in real time. Therefore, sensors developed for effective detecting changes of DPA levels in spores should be fast in response and can be long-termly operated, which may provide an immediate response to DPA concentration fluctuations. In practice, however, monitoring DPA concentration fluctuations during spores germination is very challenging. In recent years, many researchers have made profound studies in this field. [8] Some methods, such as chromatography [9] and surface-enhanced Raman technology [10], have been developed to detect DPA. Although DPA concentration can be accurately detected by these methods, it was

**Electronic supplementary material** The online version of this article (<https://doi.org/10.1007/s00604-020-04272-0>) contains supplementary material, which is available to authorized users.

✉ Minghui Yang  
yangminghui@csu.edu.cn

<sup>1</sup> Hunan Provincial Key Laboratory of Micro & Nano Materials Interface Science, College of Chemistry and Chemical Engineering, Central South University, Changsha 410083, China

hard to achieve rapid on-site detection due to the cumbersome operation procedures of these traditional methods. Fluorescence detection has a great advantage compared with these methods due to its convenience and relative rapidity. [11, 12]

Quantum dots are widely used in the fields of photocatalysis, photoluminescence, and photoelectric conversion due to quantum restriction effect. For example, carbon quantum dots have been used to detect anthrax markers, although the detection range was not wide enough and still needs to be further improved, it has inspired good ideas [13, 14]. Compared with traditional organic luminous materials, quantum dots exhibit brilliant advantages including continuous excitation spectrum, symmetrical emission spectrum, high luminous efficiency, and very strong anti-light bleaching ability [15]. Moreover, as a result of large stoker displacement, the spectral overlap between fluorescence emission and excitation can be significantly avoided, and the detection sensitivity and stability of the fluorescence signal can be improved through quantum dots [13]. Due to the effect of quantum confinement, the size and chemical composition of quantum dots can be controlled through synthesis process, and nanoparticles with emission spectrum from visible light to near-infrared region can be obtained under a single excitation light source [16, 17]. Among them, water-dispersed CdS QDs with high quantum yield have shown great potential application value in many fields, such as biological imaging, water-phase ion detection, and especially bioluminescence labeling [18].

Traditional methods for quantum dots synthesis were almost carried out in organic phase. A lot of research has been devoted to develop new methods in order to increase their practical applications, mainly including the modification of ligands on the surface of quantum dots [19]. Commonly used ligands include sulfhydryl group stabilizers and chitosan. As a stabilizer, thioglycolic acid exhibits ability of modifying carboxylic groups on the surface of CdS quantum dots, increasing their water-solubility and providing active sites for reaction [20, 21]. It has been reported that the luminescence of quantum dots with a modified surface can be quenched by transition metal ions due to electron transfer and agglomeration, which were mostly irreversible [22, 23]. However, after quenching by lanthanide ions, it was found that the fluorescence could be restored, which was a reversible process [24].

Coincidentally, particularly strong coordination between lanthanide ions and DPA has been reported [25]. Especially, compared with  $Tb^{3+}$ ,  $Eu^{3+}$  has obvious advantages in eliminating second-order scattering interference and long-wavelength red light emission of visible spectrum. Coordination water will be replaced by the tridentate ligand of DPA in the solution to form Eu-DPA chelate, which is more stable [26].

This concept inspired us to design a novel fluorescent probe to detect DPA in spores based on CdS quantum dots

stabilized by thioglycolic acid. Briefly, the surface of CdS quantum dots prepared in water system was modified with a large number of carboxylic groups. After europium ions were added into the system, fluorescence quenching of quantum dots was caused by electron transfer and agglomeration, which was a reversible process. DPA was then added to the system to compete with cadmium sulfide for europium ions, and the electron transfer process on the surface of the quantum dot was terminated, the quantum dot was also dispersed evenly again, leading to fluorescence recovery. Under optimized experimental conditions, the probe exhibits a stable response for DPA over a concentration ranging from 1 to 120  $\mu M$ , with a detection limit of 0.2  $\mu M$ . It is worth noting that this probe has good specificity for DPA, and the fluorescence of quantum dots was almost completely recovered with the increase of DPA concentration.

## Experimental

### Materials and reagents

Thioglycolic acid, sodium hydroxide, and sodium sulfide was bought from Macklin. Benzoic acid, terephthalic acid, dodecylamine, and isophthalic acid were purchased from Tokyo Chemical Industry Co., Ltd. (<https://www.tcichemicals.com/>). 2,6-Pyridinedicarboxylic acid, 2-dipicolinic acid,  $Cd(NO_3)_2 \cdot 4H_2O$  and  $Eu(NO_3)_3 \cdot 6H_2O$  were obtained from Sigma-Aldrich (<https://www.sigmaaldrich.com/>). *Bacillus subtilis* (reference number ATCC6633) were acquired from Shanghai Luwei Technology Co. Ltd. (Shanghai, China, <http://www.luweibio.com/>). All other reagents were of analytical grade and used without further purification. Ultra-pure water was used throughout all experiments.

### Apparatus

Transmission electron microscope (TEM) characterization was performed on a Tecnai G2 F20 S-TWIN TMP microscopy. The fluorescence spectra and relative fluorescence intensity (FL) were recorded on a F-7000 spectrofluorometer (Hitachi, Japan) with a fixed excitation of 460 nm. Absorption spectra were recorded on a Shimadzu UV-2450 spectrophotometer. Fourier infrared spectra (FTIR) were scanned on a Bruker Vertex 70 FTIR spectrophotometer. X-ray diffraction (XRD) was recorded on an Empyrean X-ray diffractometer.

### Preparation of TGA-CdS QDs

The thioglycolic acid capped CdS QDs (TGA-CdS QDs) were synthesized according to a previously reported method [27].

Briefly, 0.1190 g  $\text{Cd}(\text{NO}_3)_2 \cdot 4\text{H}_2\text{O}$  was dissolved in 50 mL ultra-pure water and 300  $\mu\text{L}$  TGA was added under stirring. The solution was then heated to boil and refluxed under nitrogen protection for 30 min. After that, the pH was adjusted to alkalinity and 5 mL of  $\text{Na}_2\text{S} \cdot 9\text{H}_2\text{O}$  (0.1 M) solution was added. The solution continued to flow back in a nitrogen atmosphere for 200 min. The final QDs products were collected by precipitation with isopropyl alcohol three times and re-dispersed in equal volume of water.

### Fluorescence detection for DPA concentration

To utilize the prepared probe for DPA concentration detection, 70  $\mu\text{L}$  of DPA with different concentrations ranging from 0 to 200  $\mu\text{M}$  were added to 200  $\mu\text{L}$  of CdS solution mixed with 30  $\mu\text{L}$  of 20  $\mu\text{M}$  europium ion solution, and fluorescence spectra were recorded immediately with excitation wavelength of 460 nm.

### Spores germination and fluorescence detection

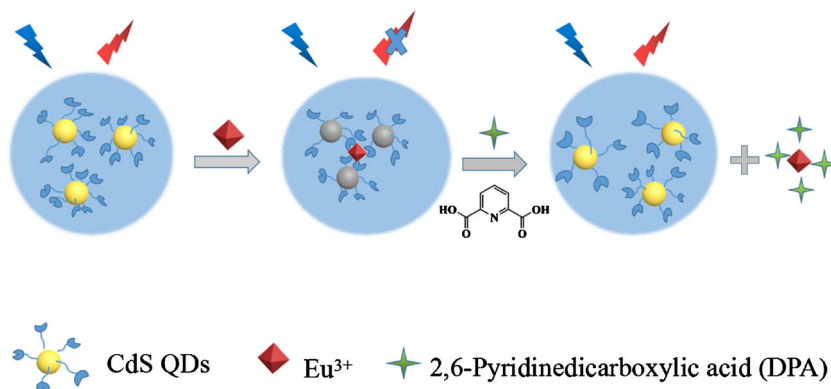
To enable spores to germination, *Bacillus subtilis* spores suspension ( $7.1 \times 10^9$  CFU $\cdot\text{mL}^{-1}$ ) was diluted to solutions with different concentrations. 2 mM of dodecylamine was added to these diluted suspension after preheating at 90  $^\circ\text{C}$  for 30 min [28]. The spores were almost germinated completely after reacting at room temperature for 30 min. After that, 70  $\mu\text{L}$  of germinated solution was added to 230  $\mu\text{L}$  of CdS-Eu mixture. Fluorescence emission spectra ranging from 500 to 800 nm were recorded immediately when excited at 460 nm.

## Results and discussion

### Design of fluorescence nanoprobe for DPA detection

As Scheme 1 shows, soluble fluorescent probe for monitoring of DPA concentration in bacterial spores was designed.

**Scheme 1** Mechanism for detection of DPA concentration

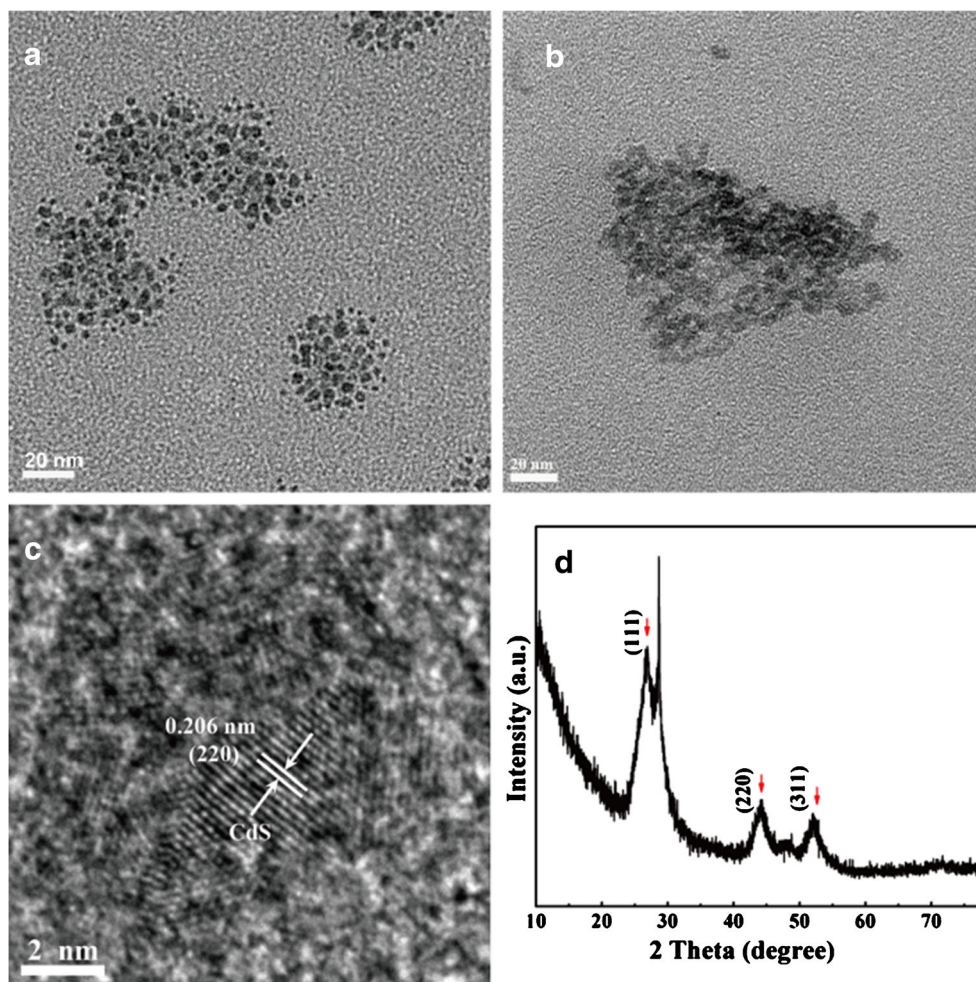


Fluorescent CdS QDs coated with thioglycolic acid were utilized as the probe due to their excellent optical properties as semiconductors, which enabling reliable detection results for biomarkers. Cationics can be used to induce fast quenching of fluorescent CdS QDs because they can combine with the carboxylic groups on the surface of quantum dots, resulting electron transfer and quantum dot aggregation. Different from irreversible quenching of quantum dot fluorescence by most other metal cations, the electron transfer of lanthanide ions occurred on the surface of quantum dot [29]. Once a new competing material was added, the quantum dot can be uniformly re-dispersed again, leading to recovery of the luminescence. So, europium ions were first added to the system to quench the fluorescence of CdS QDs. After the addition of DPA, DPA competed with CdS QDs for  $\text{Eu}^{3+}$  as the tridentate ligand of DPA has a stronger coordination effect on  $\text{Eu}^{3+}$  [30]. It enabled quick recovery of the fluorescence of quantum dots, even to the intensity before quenching, which provided a way for realizing high selective detection of DPA concentration in bacterial spores.

### Preparation and characterization of fluorescent probe

CdS quantum dots stabilized by thioglycolic acid were synthesized by a classical hydrothermal method. The transmission electron microscope (TEM, Fig. 1a, c) images and the particle size distribution (Fig. S1) show morphology of the synthesized quantum dots, which are spherical and uniformly dispersed with an average particle size of about 2.7 nm. Further characterization of CdS was performed using powder X-ray diffraction (PXRD, Fig. 1d). It can be clearly seen that three strong diffraction peaks appeared at the positions of  $2\theta = 26^\circ$ ,  $2\theta = 44^\circ$ , and  $2\theta = 51^\circ$ , which correspond to three crystal planes of (111), (220), and (331) in the cubic structure of CdS, respectively [31]. These proved the synthesized CdS was a cubic zinc structure. To ascertain that the solvothermal synthesis technique indeed produced TGA-capped CdS QDs, the prepared CdS QDs was further characterized by Fourier-transform

**Fig. 1** **a, b** TEM images of CdS QDs and CdS-Eu<sup>3+</sup> complex. **c** HR-TEM images of CdS QDs. **d** XRD pattern of CdS QDs



infrared spectroscopy (FTIR) (Fig. S2a). The FTIR broad absorption peaks at  $3382\text{ cm}^{-1}$  in the spectrum of CdS QDs is the stretching vibration peak of O-H bond. The peaks at  $2930$  and  $2853\text{ cm}^{-1}$  are assigned to the stretching and bending of  $\text{CH}_2$ , and the two peaks at  $1635$  as well as  $1386\text{ cm}^{-1}$  in the FTIR spectrum are attributed to the vibrations of C=O bond. Meanwhile, no characteristic peaks of the S-H bond are observed between  $2600$  and  $2550\text{ cm}^{-1}$ , indicating that the S-H bond is broken in thioglycolic acid, that is TGA is successfully modified on the surface of cadmium sulfide nanoparticles [32, 33]. Fluorescence spectrum and ultraviolet spectrum were utilized to record optical properties of CdS quantum dots (Fig. S2b). The excitation peak appeared around  $460\text{ nm}$ , which is basically consistent with the absorption peak (Fig. S2c). Luminescence intensity at  $650\text{ nm}$  is observed when excited at  $460\text{ nm}$ . Moreover, luminescence intensity is contiguously monitored for 10 min and recorded for 5 weeks at intervals. As shown in Fig. S2d, although the fluorescence quenching of CdS is nearly 18% after 5 weeks, the fluorescence emission intensity remains basically unchanged within dozens of minutes, which satisfied the determination of DPA content within 30 min during spores germination.

### Optimization of experimental parameters

To prove that the fluorescence quenching after adding europium ions was caused by aggregation, TEM images were also taken for CdS-Eu<sup>3+</sup> complex (Fig. 1a, b). Under the same magnification, it is obvious that quantum dots changed from the original uniform dispersion to aggregation state. To further study the effect of concentration of europium ions on the fluorescence quenching of CdS, various concentrations of europium ions were mixed with quantum dot solution and the change of fluorescence intensity was immediately recorded. With the increase of Eu<sup>3+</sup> concentration, fluorescence intensity of CdS decreased significantly, and remained stable until the concentration of Eu<sup>3+</sup> reached  $20\text{ }\mu\text{M}$ , which was therefore chosen as the optimal concentration of Eu<sup>3+</sup> (Fig. 2a).

Stern–Volmer equation was also used to analyze the quenching process [34].

$$\frac{I_0}{I} = 1 + K_{\text{SV}}[Q] \quad (1)$$

Where  $I_0$  and  $I$  are the fluorescence intensity in the absence and presence of Eu<sup>3+</sup>.  $K_{\text{SV}}$  is the quenching constant and  $[Q]$  is

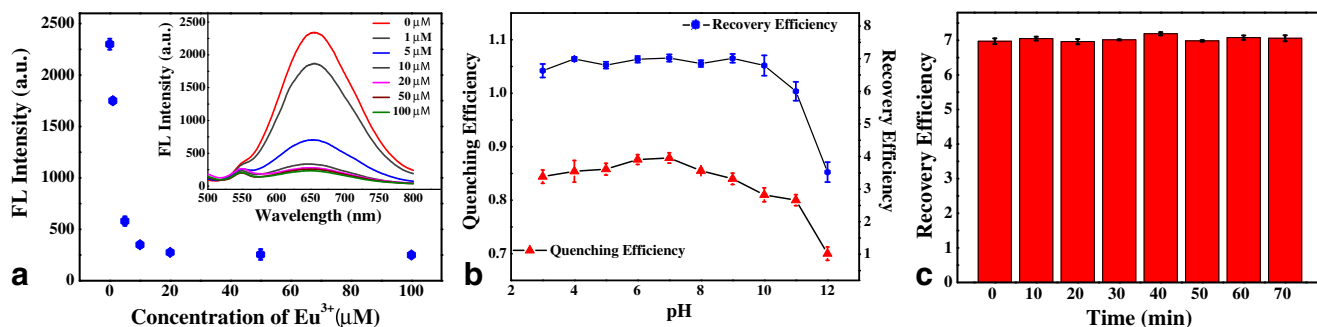


**Fig. 2** **a** Fluorescence intensity of CdS QDs with the increase of europium ions concentration. The inset is fluorescence spectra of CdS QDs mixed with different concentrations of  $\text{Eu}^{3+}$ . **b** Fluorescence quenching efficiency of  $20 \mu\text{M}$   $\text{Eu}^{3+}$  for CdS QDs (red dots) and

fluorescence recovery efficiency of  $100 \mu\text{M}$  DPA for CdS- $\text{Eu}^{3+}$  complex (blue dots) in different pH values. **c** Fluorescence recovery efficiency with time extension after adding  $100 \mu\text{M}$  DPA. Error bars show standard deviations ( $n = 3$ )

the concentration of the quencher. From the Stern-Volmer curve (Fig. S3), it can be seen that when the concentration of europium ion is lower than  $10 \mu\text{mol}$  per liter, the linear relationship is good, while when the concentration of europium ion is higher, the curve begins to curve towards the  $X$ -axis and the correlation coefficient decreases. This means that the fluorescence quenching of europium ion on the quantum dots only occurs on the surface, so the fluorescence cannot be completely quenched. So the modified Stern-Volmer equation was used to analysis the quenching data [35].

$$\frac{I_0}{I_0 - I} = \frac{1}{fK[Q]} + \frac{1}{f} \quad (2)$$

Where  $f$  is the fraction of accessible fluorophore. The dependence of  $I_0/I_0 - I$  on the reciprocal of  $\text{Eu}^{3+}$  concentration is linear (Fig. S4). The  $K_{SV}$  was calculated to be  $4.35 \times 10^5 \text{ M}^{-1}$ . And the value  $1/f$  is fixed on the ordinate so the  $f$  was calculated to be 91%. The incubation time of the CdS- $\text{Eu}^{3+}$  complex with DPA and pH of the solution were also studied to further determine the optimal reaction conditions (Fig. 2b, c).

For determination of  $100 \mu\text{M}$  DPA, the results show that there is little difference in quenching efficiency between pH 5 and 7, but the maximum recovery efficiency is achieved between pH 6 and 7 after DPA was mixed with the probe. So water solution with pH of 7 was chosen for the following experiments. It is worth noting that the fluorescence of the quantum dots recovered immediately after the DPA was mixed with the probe and remained stable for a certain period of time, which provided the conditions for real-time determination for DPA.

### Sensitivity of CdS QDs for DPA fluorescence determination

The response of the CdS- $\text{Eu}^{3+}$  complex to different concentrations of DPA was then recorded to test the linear range of the assay to DPA. The higher the concentration of DPA, the stronger the fluorescence recovery at 650 nm, indicating a DPA concentration-dependent response of the fluorescent probe. The fluorescence intensity at 650 nm was linearly proportional to DPA concentration ranging from 1 to  $120 \mu\text{M}$  (Fig. 3a, b), with a detection limit of

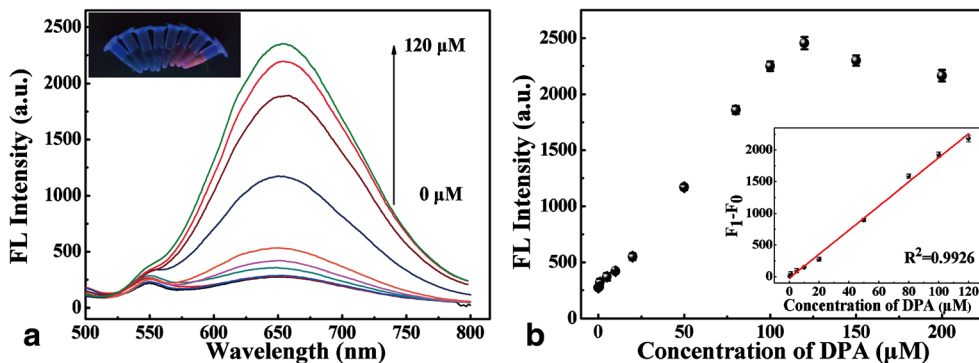


**Fig. 3** **a** Fluorescence intensity as a function of DPA concentration ranging from 0 to  $120 \mu\text{M}$ . The inset is photo for probe-DPA taken under the ultraviolet lamp with increased concentration of DPA from left to right. **b** Optimized detection range of this assay on DPA (inset) the linear

range of the probe to DPA. Fluorescence emission at 650 nm was acquired to draw the calibration plot. Each sample was measured three times ( $n = 3$ )

**Table 1** Comparison for the designed assay and other fluorescence detection methods

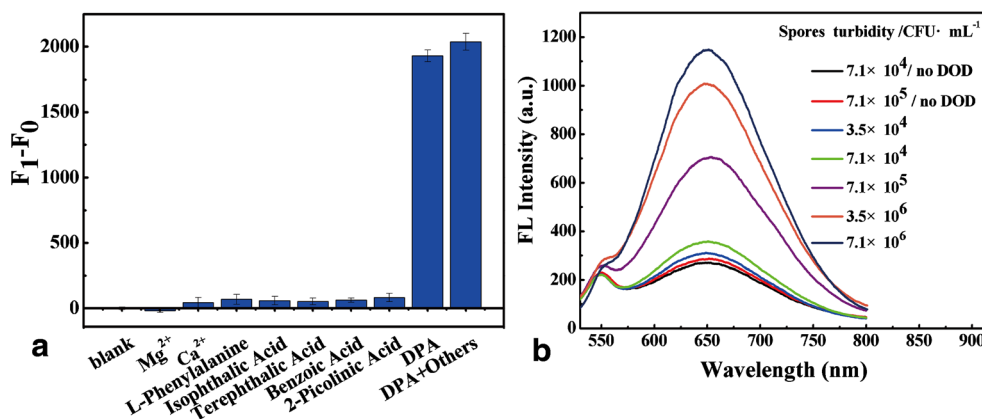
Composition of probe	Limit of detection	Linear range	Reference
Hydroxyapatite	0.077 $\mu\text{M}$	0.1–40 $\mu\text{M}$	[36]
Silver nanoparticles	0.01 $\mu\text{M}$	0.04–10 $\mu\text{M}$	[37]
Metal organic framework	0.04 nM	1 nM–5 $\mu\text{M}$	[38]
Au@glutathione	0.426 $\mu\text{M}$	1–4 $\mu\text{M}$	[39, 40]
CdS QDs	0.2 $\mu\text{M}$	1–120 $\mu\text{M}$	This work

0.2  $\mu\text{M}$  ( $3\sigma/S$ ). The test results were verified by the classical colorimetric method, which were performed using ammonium iron(II) sulfate and ascorbic acid for detection of DPA (data was shown in Supporting Information, Fig. S5). Compared with other similar monitoring methods, our method has a wider linear range and a relatively lower detection limit (Table 1). In addition, with the change of DPA concentration, the color of the probe will change significantly under the ultraviolet lamp, which provides the conditions for rapid detection.

### Specificity for DPA detection

Specificity is a vital index to evaluate the performance of a new method. To verify specificity of the probe for DPA detection, 1 mM of several common metal cations and aromatic compounds with similar structure to the DPA were incubated respectively with the probe under same conditions. Figure 4a shows responses of the probe to these materials can be nearly ignored relative to 100  $\mu\text{M}$  DPA. Even if these compounds were mixed with DPA, fluorescence emission intensity is almost not affected. These results proved that the CdS-Eu<sup>3+</sup> fluorescent probe in this work is specific for DPA detection, indicating the possibility of practical application.

**Fig. 4** **a** Fluorescence intensity changes for adding 100  $\mu\text{M}$  DPA and 1 mM of other interferences. **b** Fluorescence spectra of this probe incubated with germinated and ungerminated spores solution with different concentrations. Error bars show standard deviations ( $n = 3$ )



### Fluorescence detection of DPA in germinated spores

Considering the practical application of the probe, the release of DPA from germinated spores was studied. *Bacillus subtilis* spores were collected ( $7.1 \times 10^9$  CFU · mL<sup>-1</sup>) and diluted to different concentrations. DPA was released after germination induced by dodecylamine (DOD) [40]. And then spores were incubated with the probe and fluorescence emission spectra were recorded immediately. As shown in Fig. 4b, spores without DOD treatment do not lead to fluorescence enhancement, while fluorescence of CdS quantum dots recovered significantly when spores germinated after treating by DOD, and the degree of fluorescence recovery is significantly increased as the concentration of spores increased. However, at present, only  $\sim 3.5 \times 10^4$  spores could be detected at the minimum, and methods that can achieve a lower detection limit are still under development.

### Conclusions

In conclusion, a sensitive off-on fluorescent probe based on CdS quantum dots was developed to detect DPA in bacterial spores. The switch of fluorescence emission of quantum dot was realized through the competition between DPA and carboxylic group on the surface of quantum dot for binding with Eu<sup>3+</sup>. The quenching and recovery efficiency are all very high. The fluorescence recovery intensity has a brilliant linear relationship with DPA concentration in a wide range of concentrations. What is more gratifying is that with the change of DPA concentration, the color of the probe will change significantly under the ultraviolet lamp, which provides the conditions for rapid prediction. The probe exhibits excellent specificity and potential value in practical application. However, the activity and stability of quantum dots in water phase still need to be enhanced, which is also a condition worth optimization.

**Acknowledgments** The authors thank the support of this work by the Hunan Provincial Science and Technology Plan Project, China (No. 2019TP1001) and Innovation-Driven Project of Central South University (2020CX002).

## Compliance with ethical standards

**Conflict of interest** The authors declare that they have no conflict of interest.

## References

- Collier RJ, Young JA (2003) Anthrax toxin. *Annu Rev Cell Dev Bi* 19(1):45–70
- Friebe S, Van der Goot FG, Bürgi J (2016) The ins and outs of anthrax toxin. *Toxins* 8(3):69
- Liu S, Zhang Y, Moayeri M, Liu J, Crown D, Fattah RJ, Wein AN, Yu Z-X, Finkel T, Leppla SH (2013) Key tissue targets responsible for anthrax-toxin-induced lethality. *Nature* 501(7465):63–68
- Zhu M, Li M, Li G, Zhou Z, Liu H, Lei H, Shen Y, Wan Y (2015) Nanobody-based electrochemical immunoassay for *Bacillus thuringiensis* Cry1Ab toxin by detecting the enzymatic formation of polyaniline. *Microchim Acta* 182(15–16):2451–2459
- Yi X, Setlow P (2010) Studies of the commitment step in the germination of spores of *Bacillus* species. *J Bacteriol* 192(13):3424–3433
- Wang S, Setlow P, Y-q L (2015) Slow leakage of Ca-dipicolinic acid from individual *Bacillus* spores during initiation of spore germination. *J Bacteriol* 197(6):1095–1103
- Moir A (2006) How do spores germinate? *J Appl Microbiol* 101(3):526–530
- Cao J, Nagl S, Kothe E, Köhler JM (2015) Oxygen sensor nanoparticles for monitoring bacterial growth and characterization of dose–response functions in microfluidic screenings. *Microchim Acta* 182(1–2):385–394
- Chenau J, Fenaille F, Ezan E, Morel N, Lamourette P, Goossens PL, Becher F (2011) Sensitive detection of *Bacillus anthracis* spores by immunocapture and liquid chromatography–tandem mass spectrometry. *Anal Chem* 83(22):8675–8682
- Cowcher DP, Xu Y, Goodacre R (2013) Portable, quantitative detection of *Bacillus* bacterial spores using surface-enhanced Raman scattering. *Anal Chem* 85(6):3297–3302
- Rong M, Liang Y, Zhao D, Chen B, Pan C, Deng X, Chen Y, He J (2018) A ratiometric fluorescence visual test paper for an anthrax biomarker based on functionalized manganese-doped carbon dots. *Sensor Actuat B Chem* 265:498–505
- Wang Q-X, Xue S-F, Chen Z-H, Ma S-H, Zhang S, Shi G, Zhang M (2017) Dual lanthanide-doped complexes: the development of a time-resolved ratiometric fluorescent probe for anthrax biomarker and a paper-based visual sensor. *Biosens Bioelectron* 94:388–393
- Wegner KD, Hildebrandt N (2015) Quantum dots: bright and versatile in vitro and in vivo fluorescence imaging biosensors. *Chem Soc Rev* 44(14):4792–4834
- Rong M, Deng X, Chi S, Huang L, Zhou Y, Shen Y, Chen X (2018) Ratiometric fluorometric determination of the anthrax biomarker 2, 6-dipicolinic acid by using europium (III) -doped carbon dots in a test stripe. *Microchim Acta* 185(3):201
- Ju M-G, Dai J, Ma L, Zhou Y, Zeng XC (2018) Zero-dimensional organic–inorganic perovskite variant: transition between molecular and solid crystal. *J Am Chem Soc* 140(33):10456–10463
- Kilina S, Velizhanin KA, Ivanov S, Prezhdo OV, Tretiak S (2012) Surface ligands increase photoexcitation relaxation rates in CdSe quantum dots. *ACS Nano* 6(7):6515–6524
- Saa L, Díez-Buitrago B, Briz N, Pavlov V (2019) CdS quantum dots generated in-situ for fluorometric determination of thrombin activity. *Microchim Acta* 186(9):657
- Zhai C, Zhu M, Pang F, Bin D, Lu C, Goh MC, Yang P, Du Y (2016) High efficiency photoelectrocatalytic methanol oxidation on CdS quantum dots sensitized Pt electrode. *ACS Appl Mater Inter* 8(9):5972–5980
- Owen J, Brus L (2017) Chemical synthesis and luminescence applications of colloidal semiconductor quantum dots. *J Am Chem Soc* 139(32):10939–10943
- Butwong N, Ngeontae W, Burakham R, Srijaranai S (2013) Detection of silver (I) ion based on mixed surfactant-adsorbed CdS quantum dots. *Microchim Acta* 180(11–12):1101–1107
- Koneswaran M, Narayanaswamy R (2016) Retraction note to: CdS/ZnS core-shell quantum dots capped with mercaptoacetic acid as fluorescent probes for Hg (II) ions. *Microchim Acta* 183(4):1519–1519
- Hosseini MS, Pirouz A (2014) Study of fluorescence quenching of mercaptosuccinic acid-capped CdS quantum dots in the presence of some heavy metal ions and its application to Hg (II) ion determination. *Luminescence* 29(7):798–804
- Liu ML, Chen BB, He JH, Li CM, Li YF, Huang CZ (2019) Anthrax biomarker: an ultrasensitive fluorescent ratiometry of dipicolinic acid by using terbium (III) -modified carbon dots. *Talanta* 191:443–448
- Li W, Zhu J, Xie G, Ren Y, Zheng Y-Q (2018) Ratiometric system based on graphene quantum dots and  $\text{Eu}^{3+}$  for selective detection of tetracyclines. *Anal Chim Acta* 1022:131–137
- Zhang Y, Li B, Ma H, Zhang L, Jiang H, Song H, Zhang L, Luo Y (2016) A nanoscaled lanthanide metal–organic framework as a colorimetric fluorescence sensor for dipicolinic acid based on modulating energy transfer. *J Mater Chem C* 4(30):7294–7301
- Carr R, Evans NH, Parker D (2012) Lanthanide complexes as chiral probes exploiting circularly polarized luminescence. *Chem Soc Rev* 41(23):7673–7686
- Chen J, Wu XJ, Yin L, Li B, Hong X, Fan Z, Chen B, Xue C, Zhang H (2015) One-pot synthesis of CdS nanocrystals hybridized with single-layer transition-metal dichalcogenide nanosheets for efficient photocatalytic hydrogen evolution. *Angew Chem Int Edit* 54(4):1210–1214
- Mi L, White AD, Shao Q, Setlow P, Li Y, Jiang S (2014) Chemical insights into dodecylamine spore lethal germination. *Chem Sci* 5(8):3320–3324
- Zhang R, Chen W (2014) Nitrogen-doped carbon quantum dots: facile synthesis and application as a “turn-off” fluorescent probe for detection of  $\text{Hg}^{2+}$  ions. *Biosens Bioelectron* 55:83–90
- Yilmaz MD, Oktem HA (2018) Eriochrome black T- $\text{Eu}^{3+}$  complex as a ratiometric colorimetric and fluorescent probe for the detection of dipicolinic acid, a biomarker of bacterial spores. *Anal Chem* 90(6):4221–4225
- Malghe YS, Lavand AB (2016) Synthesis of C/ZnO/CdS nanocomposite with enhanced visible light photocatalytic activity. *Adv Mater* 7(3):239–245
- Larkin P (2011) Infrared and Raman spectroscopy: principles and spectral interpretation. Stamford, CT, USA
- Vikraman AE, Jose AR, Jacob M, Kumar KG (2015) Thioglycolic acid capped CdS quantum dots as a fluorescent probe for the nanomolar determination of dopamine. *Anal Methods* 7(16):6791–6798
- Kuijpers KPL, Bottecchia C, Cambié D, Drummen K, König NJ, Noel T (2018) A fully automated continuous-flow platform for fluorescence quenching studies and Stern-Volmer analysis. *Angew Chem Int Edit* 130:11448–11452
- Hu YJ, Liu Y, Pi ZB, Qu SS (2005) Interaction of cromolyn sodium with human serum albumin: a fluorescence quenching study. *Bioorg Med Chem* 13:6609–6614

36. Li Y, Li X, Wang D, Shen C, Yang M (2018) Hydroxyapatite nanoparticle based fluorometric turn-on determination of dipicolinic acid, a biomarker of bacterial spores. *Microchim Acta* 185(9):435
37. Tan H, Li Q, Ma C, Song Y, Xu F, Chen S, Wang L (2014) Lanthanide-functionalized silver nanoparticles for detection of an anthrax biomarker and test paper fabrication. *J Nanpart Res* 16(1): 2151
38. Bhardwaj N, Bhardwaj S, Mehta J, Kim K-H, Deep A (2016) Highly sensitive detection of dipicolinic acid with a water-dispersible terbium-metal organic framework. *Biosens Bioelectron* 86:799–804
39. Baig MMF, Chen Y-C (2019) Gold nanocluster-based fluorescence sensing probes for detection of dipicolinic acid. *Analyst* 144(10): 3289–3296. <https://doi.org/10.1039/C9AN00240E40>
40. Setlow P (2014) Germination of spores of *Bacillus* species: what we know and do not know. *J Bacteriol* 196(7):1297–1305

**Publisher's note** Springer Nature remains neutral with regard to jurisdictional claims in published maps and institutional affiliations.